JOURNAL OF OPTOELECTRONICS AND ADVANCED MATERIALS Vol. 18, No. 7-8, July - August 2016, p. 595 - 601

High performance characteristics of dual pumped Er^{+3}/Yb^{3+} Co-doped/Raman hybrid optical amplifier

O. MAHRAN[a], MOUSTAFA H. ALY[b*]
[a]*Faculty of Science, Physics Department, Alexandria University, Mohram Bey 21511, Alexandria, Egypt*
[b]*College of Engineering and Technology, Electronics and Communications Engineering Department, Arab Academy for Science, Technology and Maritime Transport Alexandria, Egypt, Member of OSA*

In this paper, a hybrid optical amplifier is suggested comprising an Er^{3+}/Yb^{3+}co-doped fiber amplifier (EYCDFA) as a pre-amplifier and a Raman fiber amplifier (RA) as a post amplifier. The performance characteristics of the hybrid amplifier (EYCDRHA) are theoretically and experimentally studied including gain and noise figure. In the theoretical model, the amplified spontaneous emission (ASE) as well as the background losses and the up-conversion effect between Er^{3+} ions and Yb^{3+} ions are taken into consideration. The performance characteristics are investigated using dual pump configuration, forward EYCDFA pump at 980 nm and backward RA pump at 1450 nm at different values of input signal power, EYCDFA and RA pump powers and lengths at two different values of input signal wavelength; 1530 and 1600 nm. A high gain and low noise performance are obtained for the suggested amplifier. Furthermore, a good agreement between the theoretical and experimental values of the gain and noise figure at the input parameters is obtained.

(Received April 20, 2016; accepted August 3, 2016)

Keywords: Optical amplifiers, Raman amplifier, Erbium doped fiber amplifier, Hybrid amplifier, Ytterbium, Pumping, Amplified spontaneous emission

1. Introduction

The phosphate as host glass has an important feature when doped by Er/Yb to form a co-doped fiber amplifier (EYCDFA). It offers a low cooperative up-conversion coefficient of the $^4I_{13/2}$ level of the Er^{3+} ions [1-3]. Many candidates reported the performance of highly Er/Yb co-doped multimode phosphate glass fibers which were used in high gain short-length amplifiers [4-6]. In Ref. [7], a single- mode highly Er/Yb co-doped phosphate glass-fiber is fabricated by rod-in tube technique. Its gain and noise figure are measured by dual-pump configuration at -30, -10 and -1 dBm input signal level. A net gain coefficient is obtained as high as 3.3 dB/cm froming a micro erbium doped fiber amplifier (EDFA) based on a 5 cm long phosphate fiber. Furthermore, when Yb^{3+} ion is doped with Er^{3+} ion in the host glass, it provides several advantages including stronger absorption band in the region 880-1050 nm and a large overlap between Yb^{3+} emission and Er^{3+} absorption which makes the EYCDFA suitable to obtain large gain [8].

The use of distributed Raman amplification in fibers can provide improved noise figure, signal power gain and optical signal to noise ratio (OSNR) [9]. The hybrid amplifier is a combination of two amplifiers for obtaining higher gain and lower noise figure than the single amplifier. EDFA/Raman with hybrid configuration has been extensively studied showing low noise figure and high gain for transmission systems compared to conventional EDFA [10-12]. Simranjit Singh and R.S. Kaler provided an analytical model of EDFA-Raman hybrid optical amplifier and optimized the various parameters using genetic algorithm method [13]. Furthermore, the L-band remote EDFA/Raman hybrid amplifier was experimentally investigated for flat gain [14].

In this paper, the performance characteristics of EYCDFA/Raman hybrid amplifier **(EYCDRHA)** are investigated experimentally and theoretically. A hybrid amplifier comprises a two- stage erbium-ytterbium co-doped fiber amplifier of length (0.5-1.2 m) at forward 980 nm pump of power (100- 500 mW) as pre-amplifier and Raman fiber amplifier of length (10- 45 km) at backward 1450 nm pump of power (50-250 mW) as a post amplifier. The input signal power varies from - 40 to 10 dBm at two different values of signal wavelength; 1530 and 1600 nm, which are the start and end points of the signal wavelength range. The proposed theoretical model takes into account the amplified spontaneous emission (ASE), the background losses and the up-conversion effect of EYCDFA.

2. Basic model

First, we consider the rate and power equations of the signal, pump and ASE in the pre-amplifier (EYCDFA), where the input signal power in EYCDFA is $P_{s1}(0)$ and the output signal power is $P_{s1}(L_{EYDFA})$. Second, we consider the power equations in the post amplifier (RA), where the input signal power is $P_{s2}(0) = P_{s1}(L_{EYDFA})$ and the output signal power is $P_{s2}(L_{RA})$, where L_{EYDFA} is the EYCDFA length and L_{RA} is the RA length. Fig. 1 represents the energy level diagram of the Er^{+3}/Yb^{3+} system.

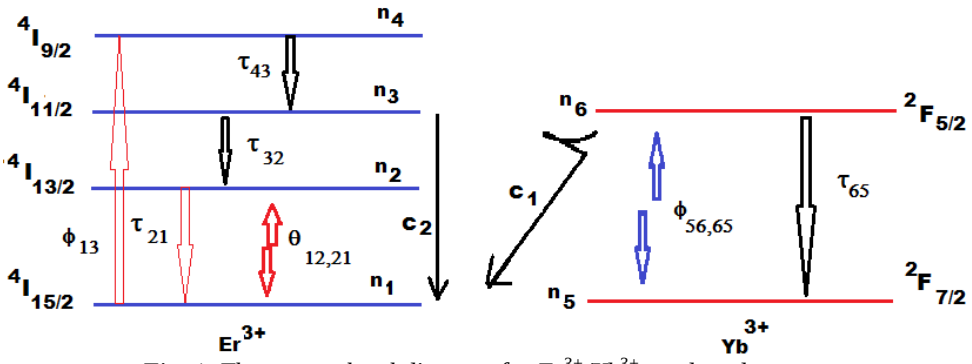

Fig. 1. The energy level diagram for Er^{3+}/Yb^{3+} co-doped system.

The theoretical model depends on the energy level diagram of EYCDF in Fig. 1. Neglecting the spontaneous emission life time between levels 4 and 3, τ_{43} and the number of Er ions in level 4, n_4, and using Ref. [15], one can get the rate equations of Er/Yb co-doped fiber amplifier as

$$\frac{dn_1}{dt} = \frac{n_2}{\tau_{21}} - \theta_{12}n_1 + \theta_{21}n_2 - \emptyset_{13}n_1 + C_2n_2^2 + C_2n_3^2 - C_1n_1n_6 \quad (1)$$

$$\frac{dn_2}{dt} = \frac{n_3}{\tau_{32}} - \frac{n_2}{\tau_{21}} - \theta_{21}n_2 + \theta_{12}n_1 - 2C_2n_2^2 \quad (2)$$

$$\frac{dn_3}{dt} = -\frac{n_3}{\tau_{32}} + \emptyset_{13}n_1 - 2C_2n_3^2 + -C_1n_3n_5 + C_1n_1n_6 \quad (3)$$

$$\frac{dn_6}{dt} = -\frac{n_6}{\tau_{65}} + \emptyset_{56}n_5 - \emptyset_{65}n_6 + C_1n_3n_5 - C_1n_1n_6 \quad (4)$$

$$n_1 + n_2 + n_3 = n_{Er} \quad (5)$$

$$n_5 + n_6 = n_{Yb} \quad (6)$$

Here, τ_{ij} refers to the spontaneous emission lifetimes between levels i and j, θ_{12} and θ_{21} are, respectively, the signal absorption and emission rates of Er^{3+}, Φ_{13} is the pump absorption rate of Er^{3+} and Φ_{56} and Φ_{65} are the pump absorption and emission rates of Yb^{3+}, respectively. C_1 and C_2 are the cross-relaxation and up-conversion coefficients, respectively. $C_2n_2^2$ and $C_2n_3^2$ are terms accounting for uniform up-conversion, and $C_1n_3n_5$and $C_1n_1n_6$ are terms representing the energy transfer between Er^{3+} to Yb^{3+} and Yb^{3+} to Er^{3+}, respectively.

The transition rates $\emptyset_{ij}$, θ_{ij} are given by [15]

$$\emptyset_{ij}, \theta_{ij} = \frac{\sigma_{ij}(\nu_{p,s})}{h\nu_{p,s}} P_{p,s}(z)\left|E(r,\nu_{p,s})\right|^2 + \int_0^\infty \frac{\sigma_{ij}(\nu_{p,s})}{h\nu_{p,s}}[P_{ASE}^+ + P_{ASE}^-].\left|E(r,\nu_{p,s})\right|^2 d\nu \quad (7)$$

where σ_{ij} is the cross-section of signal and pump, ν_s and ν_p are the signal and pump frequencies, respectively, h is the Planck's constant, P_s and P_p are the signal and pump powers, respectively, $P_{ASE}^{\pm}(z,\nu)$ are the forward (plus sign) and backward (minus sign) ASE powers, respectively, at a frequency ν in a frequency interval Δν and at the longitudinal fiber coordinate z. E(ν, r) is the field distribution of the LP_{01} mode.

The value of E(ν, r) can be obtained through normalization as [16]

$$2\pi \int_0^\infty \left|E(r,\nu_{p,s})\right|^2 r\, dr = 1 \quad (8)$$

The power propagation equations along the EYDF for signal, pump and ASE are given as [16]

$$\frac{dP_{s1}(z)}{dz} = [\Gamma_{s1}(\nu_{s1})\{\sigma_{21}(\nu_{s1})n_2(z) - \sigma_{12}(\nu_{s1})n_1(z)\} - \alpha_{s1}(\nu_{s1})]P_{s1}(z) \quad (9)$$

$$\frac{dP_{p1}(z)}{dz} = \left[\Gamma_{p1}(\nu_{p1})\{\sigma_{65}(\nu_{p1})n_6(z) - \sigma_{56}(\nu_{p1})n_5(z) - \sigma_{13}(\nu_{p1})n_1(z)\} - \alpha_{p1}(\nu_{p1})\right]P_{p1}(z) \quad (10)$$

$$\frac{dP_{ASE}^{\pm}(z)}{dz} = \pm h\nu_{p1}\Delta\nu\Gamma_{p1}(\nu_{p1})\sigma_{65}(\nu_{p1})n_6(z). \left[\Gamma_{p1}(\nu_{p1}).\{\sigma_{65}(\nu_{p1})n_6(z) - \sigma_{56}(\nu_{p1})n_5(z)\} - \alpha(\nu)\right]P_{ASE}^{\pm}(z) \quad (11)$$

where $\alpha(\nu_{s1})$, $\alpha(\nu_{p1})$ and $\alpha(\nu)$ are the frequency-dependent background losses at the signal, pump and ASE bandwidth, Γ_s and Γ_p are the overlapping factors of the light signal and pump light, respectively. σ_{12} (ν_s), σ_{21} (ν_s) and σ_{13} (ν_p) are the emission/absorption cross-sections at the optical frequency ν for the Er^{3+} while σ_{54} (ν_p) and σ_{45} (ν_p) are the emission and absorption cross-sections for the Yb^{3+}.

The output signal from the pre-amplifier and noise figure are, respectively, given by [15-18]

$$P_{s1}(L_{EYDFA}) = G_{EYDFA}P_{s1}(0) \quad (12)$$

$$NF_{EYDFA} = \frac{1}{G_{EYDFA}} + \frac{P_{ASE}^{\pm}(\nu,z)}{G_{EYDFA}h\nu_s\Delta\nu_s} \quad (13)$$

where G_{EYDFA} is the gain of the pre-amplifier (EYCDFA).

For Raman amplifier, the rate equation can be written as [19]

$$\frac{dP_{s2}(z)}{dz} = -\alpha_{sR}P_{s1} + \frac{g_RP_{pR}P_{s1}}{\gamma_p} \quad (14)$$

$$-\frac{dP_{pR}}{dz} = -\alpha_{pR}P_{pR} + \frac{f_{pR}}{f_{sR}}\frac{g_R P_{pR} P_{s1}}{\gamma_p} \quad (15)$$

where P_{s2} is input signal power for Raman amplifier, which is the also the output signal power of EYCDFA, g_R is Raman gain coefficient, P_{pR} is the pump power for Raman amplifier, γ_p is the cross-sectional area of pump beam inside the fiber, α_{sR} and α_{pR} is fiber losses at signal and pump at frequencies f_{sR} and f_{pR}. The negative sign indicates the backward pumping.

The Raman gain coefficient is calculated from the relation [20]

$$g_R = \gamma_s(\nu)\frac{\lambda_s^3}{c^2 h(n(\nu))^2} \quad (16)$$

γ_s is the Raman cross section of the signal, λ_s is the Stokes wavelength and n(ν) is the frequency dependent refractive index.

The gain of Raman amplifier is given as

$$G_{Raman} = 10\, log_{10}\{\frac{P_{s2}(L_{Raman})}{P_{s1}(L_{EYDFA})}\} \quad (17)$$

Now, the noise figure of Raman can written as [19]

$$NF_{Raman} = \frac{2(\bar{P_{ASE}})Raman}{h\nu_{sr}\Delta\nu_r G_{Raman}} + \frac{1}{G_{Raman}} \quad (18)$$

where $\Delta\nu_r$ is the reference optical bandwidth corresponding to 0.1 nm [21, 22].

The gain of EYCDFA/Raman hybrid amplifier (EYCDRHA), G_{HA}, is given by [20]

$$G_{HA} = 10\, log_{10}(\frac{P_{s2}(L_{Raman})}{P_{s1}(0)}) \quad (19)$$

and the net noise figure for the EYCDRHA is [19]

$$NF_{HA} = \frac{1}{G_{EYDFA}} + \frac{P_{ASE}^{\pm}(\nu,z)}{G_{EYDFA}h\nu_s\Delta\nu_s} + \frac{NF_{Raman}-1}{G_{EDFA}} \quad (20)$$

3. Numerical analysis

The results of theoretical model are obtained by solving Eqs. (9)-(11) for the EYCDFA at different values of pump and signal powers. The boundary conditions are taken as $P_{p1}(z=0) = P_{p1}$ = (100-500 mW), $Ps1(0) = P_{s1}$ = (-40 to +10 dBm) and $P_{ASE}^{+}(z=0,\nu) = P_{ASE}^{-}(z = L_{EYDFA},\nu)$. The solution of the rate equations Eqs. (1)-(6) is obtained under the condition $dn_i/dt = 0$ and the numerical solution of the equations is performed using Runge-Kutta iterative procedure. The output signal $P_{s1}(L_{EYDFA})$ of EYCDFA is considered as input signal $P_{s2}(0)$ for Raman amplifier.

Equations (14) and (15) are solved using the cross section evaluated in Eq. (16), with boundary conditions $P_{pR}(z=0) = P_{pR}$ = (50-250 mW) to obtain the output signal of Raman amplifier $P_{s2}(L_{Raman})$. Now, we can find the gain and noise figure of hybrid amplifier using Eqs. (19) and (20). For each operating wavelength, the absorption and emission of both Er and Yb in the EYD phosphate glass in Ref. [23] are used and the cross section of Raman fiber in Ref. [20, 24] is used in Eq. (16). All input parameters used in the theoretical model for EYCDFA and Raman amplifier are listed in Tables 1-3.

Table 1. EYCDRHA [19-23].

Parameter	Symbol	Value	Unit
Raman pump power	P_{pR}	(50-250)	mW
EYDFA pump power	P_{p1}	100 – 500	mW
RA length	L_R	10-45	km
EYDFA length	L_{EYDFA}	0.5 - 1.2	m
Number of input signal channels	N_{in}	70	-
Number of output signal channels	N_{out}	70	-

Table 2. EYCDFA parameters [15-18].

Parameter	Symbol	Value	Unit
Pump wavelength	λ_p	980	nm
Signal wavelength	λ_s	1530	nm
Er concentration	N_{Er}	5.14×10^{25}	m^{-3}
Yb concentration	N_{Yb}	6.2×10^{26}	m^{-3}
Er^{3+} absorption cross-section	σ_{13}	2.58×10^{-25}	m^2
Yb^{3+} absorption cross-section	σ_{45}	1.0×10^{-24}	m^2
Yb^{3+} emission cross-section	σ_{54}	1.0×10^{-24}	m^2
Er^{3+} absorption cross-section	σ_{12}	6.5×10^{-25}	m^2
Er^{3+} emission cross-section	σ_{21}	7.0×10^{-25}	m^2
Er^{3+} emission lifetime	τ_{21}	10	ms
Yb^{3+} emission lifetime	τ_{65}	1.5	ms
Life time	τ_{32}	10^{-9}	s
Cross-relaxation coefficient	C_1	3.44×10^{-22}	m^3/s
Up-conversion coefficient	C_2	5.2834×10^{-22}	m^3/s
Core radius	a	2	μm
Doping radius	r	2	μm
Numerical aperature	NA	0.15	-
Core refractive index	n_1	1.52812	-
Cladding refractive index	n_2	1.51	-
Amplifier cross-section	A_{eff}	50	μm^2
Pump overlap factor	Γ_p	0.921	-
Signal overlap factor	Γ_s	0.795	-
Signal loss	α_{s1}	0.1	dB/m
Pump loss	α_{p1}	0.15	dB/m
Amplified spontaneous emission	$P_{ASE}^{+}(0)$	0.15	mW

Table 3. RA parameters [19-23].

Parameter	Symbol	Value	Unit
Raman gain coefficient	g_R	10×10^{-14}	-
Reference optical bandwidth	$\Delta\nu_r$	0.1	nm
Pump wavelength	λ_{pR}	1450	nm
Fiber loss at signal frequency	α_{sR}	2.3×10^{-5}	dB/m
Fiber loss at pump frequency	α_{pR}	2.33×10^{-5}	dB/m
Cross-sectional area of pump beam	γ_s	10.2×10^{12}	m^2
Cross-sectional area of signal beam	γ_p	11.5×10^{12}	m^2
Amplified spontaneous emission	$P^{+}_{ASE}(0)$	0.22	mW

4. Experimental setup

Fig. 2 shows the EYCDRHA experimental setup, designed by Optisystem ver.7.1. The system consists of 70 channels covering the wavelength range 1525-1610 nm. This is performed using a continuous wave (CW) laser array. The 980 nm pump laser used for EYCDFA is of 300 mW forward with multiplexed signals through the pump coupler. An erbium-ytterbium doped phosphate glass fiber is chosen at lengths of 0.7-1 m. The output of EYCDFA is directed from the isolator to a Raman phosphate based glass of lengths 25 km. The Raman amplifier is backward pumped with 200 mW at 1450 nm. The output signals are demultiplexed by fiber Bragg gratings and are recorded by the optical receiver.

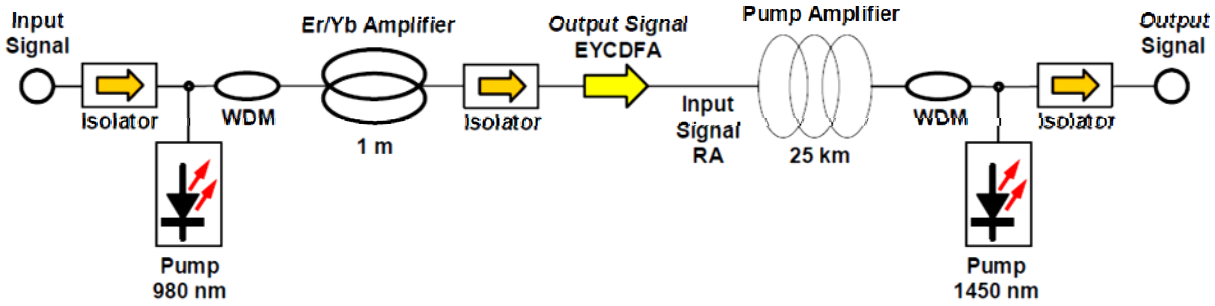

Fig. 2. Hybrid EYCDFA/Raman amplifier setup.

5. Results and discussion

Fig. 3 shows the obtained gain theoretically and experimentally of the EYCDRHA as a function of input signal power at RA length of 25 km and pump power of 200 mW, Er/Yb co-doped amplifier length of 1m and pump power of 500 mW, at two different values of signal wavelengths 1530 and 1600 nm, respectively.

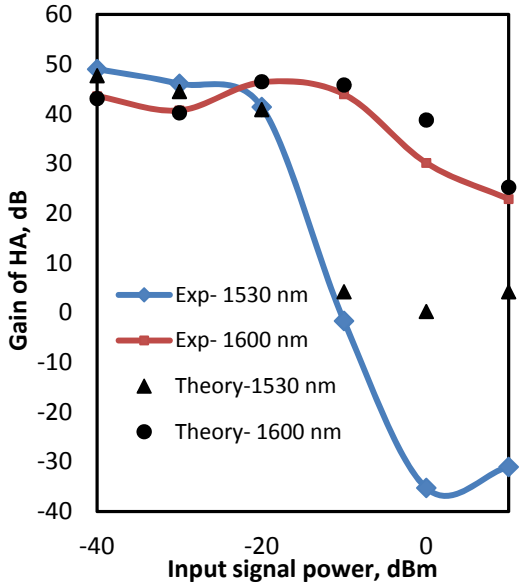

Fig. 3. Gain of HA versus the input signal power.

At 1530 nm, it is clear that, the gain has a maximum value 49 dB at - 40 dBm signal power, and the gain is positive for input signal power < 10 dBm. A good agreement is noticed between the theoretical and experimental results of the gain.

The gain becomes negative for more increase in signal power > - 10 dBm where in this range of input signal power, the theoretical values of the gain display 0.2 dB at 0 dBm and 4.2 dB at -10 dBm. The difference between the theoretical and experimental results at the two signal powers 0 and 10 dBm is due to the values of loss coefficients and ASE in the theoretical model which are considered.

At 1600 nm, the gain is positive for all values of the input signal power and has a maximum value of 43 dB at - 40 dBm signal power. There is also a fair agreement between experimental and theoretical results, except at 0 dBm signal power, the theoretical gain exceed 8 dB than the experimental gain value due to the loss and ASE effects that are considered in the theoretical model.

The theoretical model is limited to positive values of gain and so there is a difference between theoretical and experimental at the values of input signal power from -10 dBm to 10 dBm

Fig. 4 shows the noise figure of EYCDRHA as a function of input signal power at the same conditions of Fig. 3. The noise figure has minimum values of (~ 3.4dB at 1530 nm) and (5 dB at 1600 nm) for input signal of - 40 dBm. The large values of noise figure are found at input

signal power > 0 dBm at 1530 nm. Furthermore, the noise figure is nearly constant for all values of input signal power at 1600 nm. There is a fair agreement between theoretical and experimental values of the noise figure at 1530 nm till -10 dBm signal power and a slight difference of the theoretical and experimental values of the noise figure at all range of input signal power at 1600 nm.

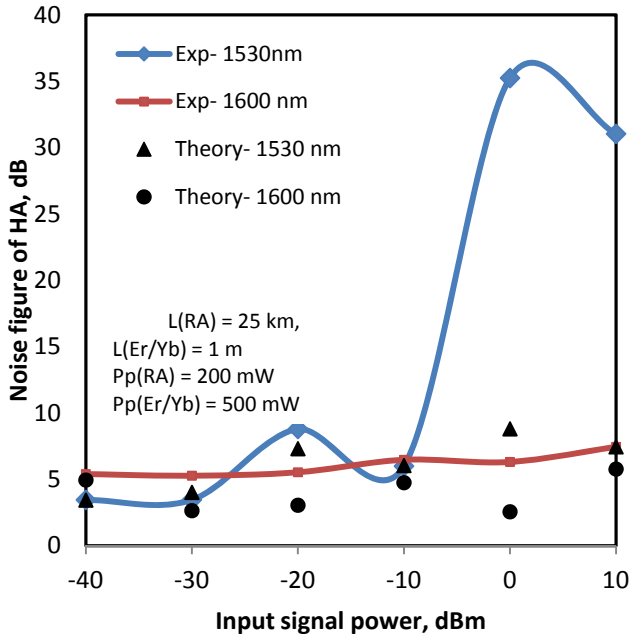

Fig. 4. Noise figure of HA versus the input signal power.

The dependence of the gain and noise figure of EYCDRHA on Er/Yb co-doped 980 nm forward pump power at - 40 dBm signal power and RA 1450 nm backward pump power at 200 mW is displayed, respectively, in Figs. 5 and 6. The Er/Yb co-doped fiber amplifier length is RA length is 25 km.

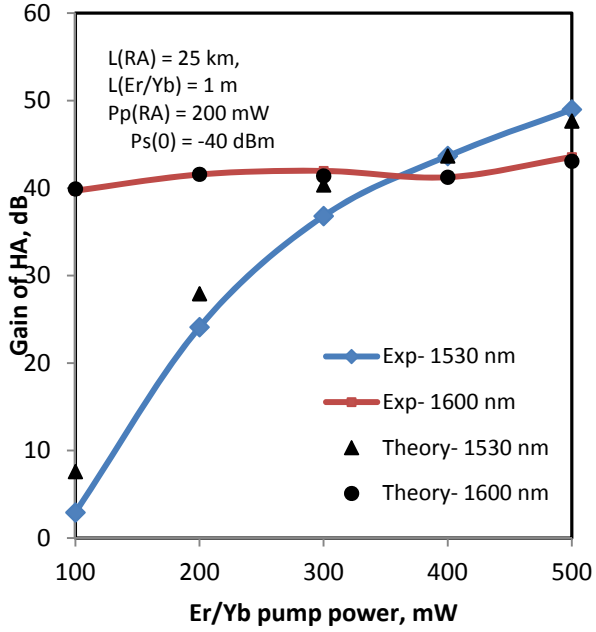

Fig. 5. Gain of HA versus Er/Yb pump power.

In Fig. 5, the gain is nearly constant at 1600 nm. This is because the gain at this range of wavelength is affected largely by the RA pump power and length, which are fixed in this case. At 1530 nm, gain increases with Er/Yb co-doped pump power. There is also a good agreement between theoretical and experimental results.

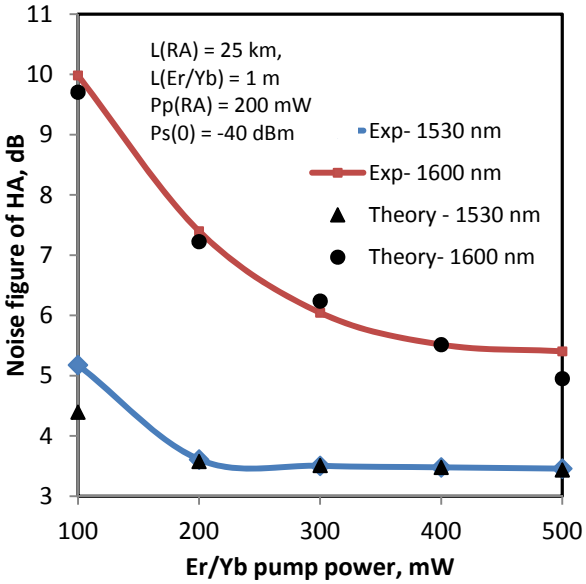

Fig. 6. Noise figure of HA versus Er/Yb pump power.

In Fig.6, the noise figure decreases with Er/Yb co-doped amplifier pump power and is then saturated at pump power > 200 mW at 1530 nm, while it decreases all over the Er/Yb co-doped pump power range at 1600 nm. The minimum value of noise figure (3.43 dB) is obtained at 500 mW at 1530 nm. Again, there is a good agreement between theoretical and experimental values of noise figure.

The effect of RA pump power on the gain and noise figure of EYCDRHA is displayed, respectively, in Figs. 7 and 8. RA pump power has the range 50-250 mW, at input signal power of -40 dBm, Er/Yb amplifier and RA lengths are 1 m and 25 km, respectively, and Er/Yb pump power is 500 mW.

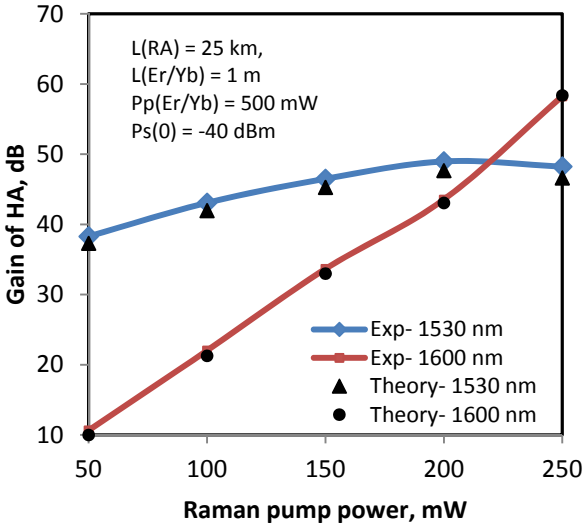

Fig. 7. Gain of HA versus RA pump power.

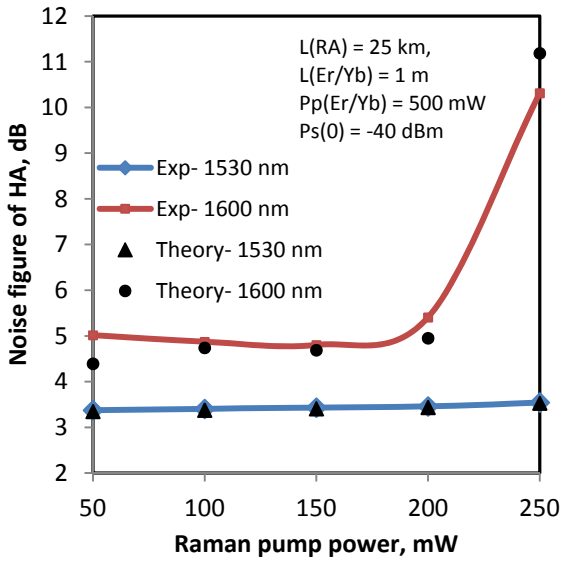

Fig. 8. Noise figure of HA versus RA power.

At 1530 nm signal wavelength, the gain increases with the RA pump power in the range < 200 mW as in Fig. 7. Then, it has a maximum value of ~ 49 dB at 200 mW, for pump > 200 mW, and then begins decreasing. There is a slight difference between experimental and theoretical results of the gain, at this wavelength. Noise figure is nearly constant at this signal wavelength as in Fig.8, and there is good agreement between experimental and theoretical results.

At 1600 nm, the gain is continuously increasing with RA pump power and the noise figure is saturated till 200 mW, then it increases with RA pump power > 200 mW as in Figs. 7 and 8, respectively. Furthermore, there is good agreement between experimental and theoretical results.

Figs. 9 and 10 display, respectively, gain and noise figure of EYCDRHA as a function of Er/Yb co-doped amplifier length.

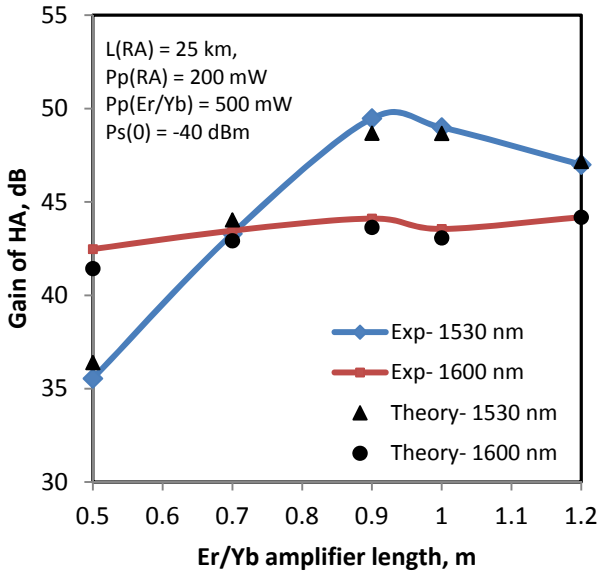

Fig. 9. Gain of HA versus Er/Yb amplifier length.

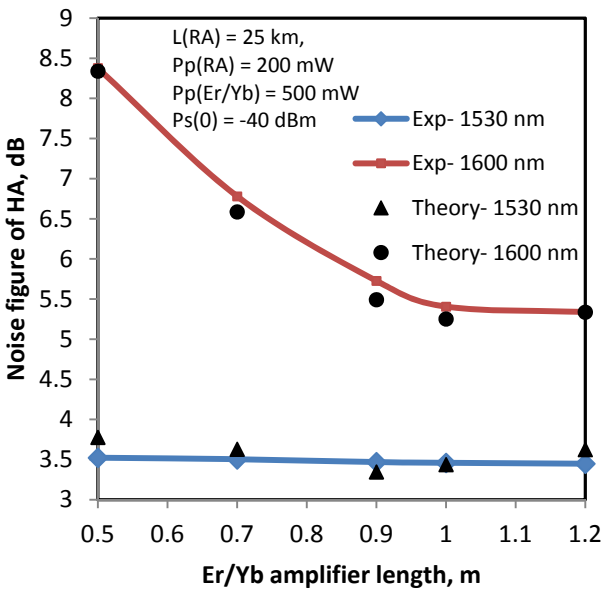

Fig. 10. Noise figure of HA versus Er/Yb amplifier length.

The input signal power is taken - 40 dBm with 25 km of RA length, and Er/Yb and RA pump power of 500 mW and 200 mW, respectively, for the selected signal wavelengths 1530 and 1600 nm.

As seen in Fig.9, both experimental and theoretical models have a maximum gain of ~ 49 dB between 0.9 and 1m of Er/Yb co-doped amplifier length, at 1530 nm with a slight change from 42 to 44 dB in the Er/Yb co-doped amplifier length range at 1600 nm. Furthermore, the experimental noise figure of Fig.10 shows a slightly decrease behavior in the amplifier length range from 3.5 to 3.4 dB at 1530 nm and a strong decease from 8.3 dB, 0.5 m to 5.2 dB, 1 m, then saturation at Er/Yb co-doped amplifier length > 1m at 1600 nm. The theoretical noise figure in Fig. 10 is slightly different from experimental values at both signal wavelengths 1350 and 1600 nm due to the same causes discussed in Fig. 3.

The gain and noise figure dependence of EYCDRHA on RA length (10-45 km) are displayed in Figs. 11and 12, respectively. The input signal power is taken - 40 dBm, Er/Yb amplifier length and pump power are, respectively, 1 m and 500 mW, RA and pump power is kept at 200 mW, for the two selected signal wavelengths 1530 and 1600 nm. At 1530 nm, the EYCDRHA gain increases with RA length till 25 km (with a maximum value of ~ 49 dB) and then decreases. At 1600 nm, the gain continuously increases with RA length.

Fig. 11 shows a good agreement between theoretical and experimental values of the amplifier gain. Noise figure of EYCDRHA, Fig. 12, shows a constant behavior around 3.4 dB as RA length increases at 1530 nm and an increasing behavior with RA length at 1600 nm. The theoretical and experimental results are nearly similar.

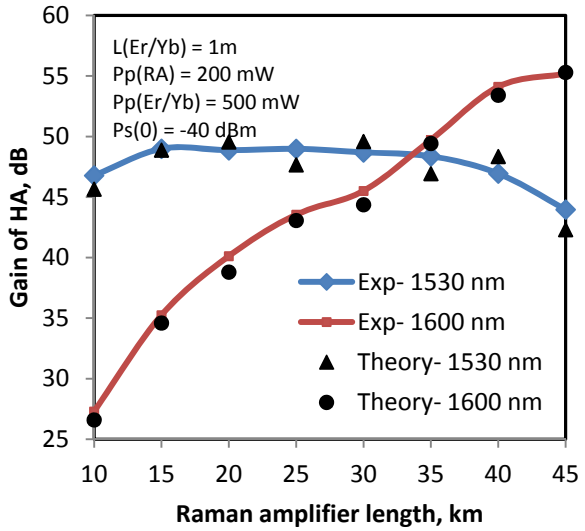

Fig. 11. Gain of HA versus RA length.

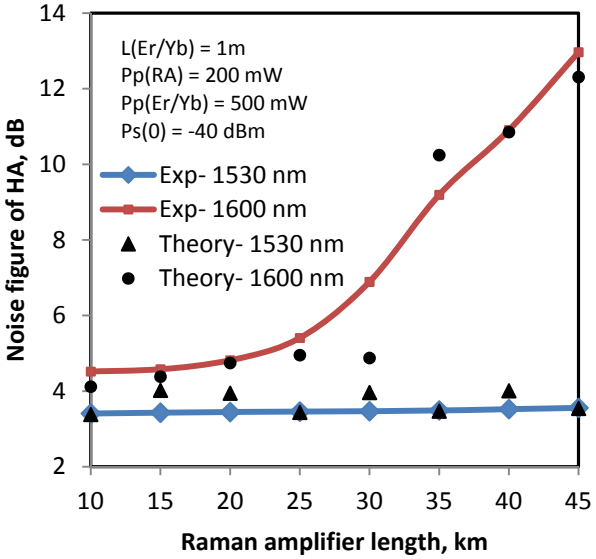

Fig. 12. Noise figure of HA versus RA length.

6. Conclusion

In this paper, we experimentally and theoretically studied a hybrid optical amplifier (HA) comprising an erbium ytterbium co-doped fiber amplifier and a Raman amplifier. The EYCDFA is used as pre-amplifier and the RA as a poster one. The effect of the amplifier parameters like length, pump power, signal power and signal wavelength on the HA performance is investigated. The ASE, background losses and the up-conversion of EYCDFA effects are taken into account in the theoretical model. A high gain of 49 dB at 1530 nm and 43 dB at 1600 nm and low noise figure of 3.4 dB at 1530 nm and 5 dB at 1600 nm are obtained. These values are yielded at input signal of - 40 dBm with EYDFA and RA pump power of 500 mW and 200 mW, EYDFA and RA lengths of 1 m and 25 km, respectively. Furthermore, a fair agreement is obtained between the experimental and theoretical values of the gain and noise figure.

References

[1] Zhuping Liu, Changhong Qi, Shixun Dai, Yasi Jiang, Lili Hu, Optical Materials, **21**, 789 (2003).
[2] H. Desirena, E. De la Rosa, L. A. Diaz-Torres, G. A. Kumar, Optical Materials, **28**, 560 (2006).
[3] E. Desurvire, Erbium Doped Fiber Amplifiers: Principles and Applications, Wiley, 1994.
[4] Yu-Hai Wang, Chun-Sheng Ma, De-Lu Li, Da-Ming Zhang, Optica Applicata, **38**, 329 (2008).
[5] Y. Jaouen, S. Bordais, E. Olmedo, G. Kulcsar, J.Y. Allain, Ann. Telecommun., **58**, 1640 (2003).
[6] F. Di Pasquale, M. Federighi, IEEE J. Quantum Electron., **30**, 2127 (1994).
[7] S. H. Xu, Z. M. Yang, Z. M. Feng, Q. Y. Zhang, Z.H. Jiang, W. C. Xu, in Proceedings of IEEE Nanoelectronics Conference, China, p. 633 (2008).
[8] O. Mahran, Australian J. Basic and Appl. Science, **9**, 84 (2015).
[9] Federica Poli, Lorenzo Rosa, Michele Bottacini, Matteo Foroni, Annamaria Cucinotta, Stefano Selleri, IEEE Photon. Technol. Lett., **17**, 2556 (2005).
[10] O. Mahran, Ahmed E. El-Samahy, H. Moustafa Aly, Mourad Abd EL Hai, Optoelectron. Adv. Mat. **9**, 575 (2015).
[11] Federica Poli, Lorenzo Rosa, Michele Bottacini, Matteo Foroni, Annamaria Cucinotta, Stefano Selleri, IEEE Photon. Technol. Lett., **17**, 2556 (2005).
[12] Ju Han Lee, You Min Chang, Young Geun Han, Haeyang Chung, Sang Hyuck Kim, Sang Bae Lee, J. Lightwave Technol., **23**, 3484 (2005).
[13] Simranjit Singh, R. S. Kaler, Optics and Laser Technol., **68**, 89 (2015).
[14] M. H. AbuBakar, F. R.MahamdAdikan, N. H.Ibrahim, M. A.Mahdi, Optics Communications, **291**, 155 (2013).
[15] Cuneyt Berkdemir, Sedat Özsoy, Optical Materials, **31**, 229 (2008).
[16] M. R. A. Moghaddam, S. W. Harun, R. Parvizi , Z. S. Salleh, H. Arof, A. Lokman, H. Ahmad, Optik, **122**, 1783 (2011).
[17] Abdel Hakeim M. Hussein, Ali H. El-Astal, Fady I. El-Nahal, Optical Materials, **33**, 543 (2011).
[18] A.Shooshtari, T.Touam, S. I Najafi, S. Safavi-Naeini, H. Hatami-Hanza, Optical and Quantum Electronics, **30**, 1998.
[19] O. Mahran, Optics Communications, **353**, 158 (2015).
[20] H. Arwa Beshr, H. Moustafa Aly, in Proceedings of 24th IEEE National Radio Science Conference, Egypt, p. D1, 2007.
[21] Jake Bromage, J. Lightwave Technol, **22**, 79 (2004).
[22] Yasuhiro Aoki, J. Lightwave Technol., **6**, 1225 (1988).
[23] C. George Valley, Optical Fiber Technol., **7**, 21 (2001).
[24] R. H. Stolen, E. P. Ippen, Appl. Phys. Lett., **22**, 276 (1973).

*Corresponding author: drmosaly@gmail.com, mosaly@aast.edu